LAWRENCE
LIVERMORE
NATIONAL
LABORATORY

LLNL-TR-481511

Fossil Fuel (CO2) Emission Verification Capability07-ERD-064 Final Report

T. P. Guilderson, P. Cameron-Smith, D. D. Lucas

April 27, 2011

Disclaimer

This document was prepared as an account of work sponsored by an agency of the United States government. Neither the United States government nor Lawrence Livermore National Security, LLC, nor any of their employees makes any warranty, expressed or implied, or assumes any legal liability or responsibility for the accuracy, completeness, or usefulness of any information, apparatus, product, or process disclosed, or represents that its use would not infringe privately owned rights. Reference herein to any specific commercial product, process, or service by trade name, trademark, manufacturer, or otherwise does not necessarily constitute or imply its endorsement, recommendation, or favoring by the United States government or Lawrence Livermore National Security, LLC. The views and opinions of authors expressed herein do not necessarily state or reflect those of the United States government or Lawrence Livermore National Security, LLC, and shall not be used for advertising or product endorsement purposes.

This work performed under the auspices of the U.S. Department of Energy by Lawrence Livermore National Laboratory under Contract DE-AC52-07NA27344.

Fossil Fuel (CO_2) Emission Verification Capability
07-ERD-064
Final Report

T. P. Guilderson, P. Cameron-Smith, D. D. Lucas

(including work on this project by B. Kosovic, L Delle Monache, and D. Bergmann)

Background

Human induced climate change as the result of the utilization and release of fossil fuel carbon is real. The domestic and international political landscape has changed such that it is recognized that there will very likely be the need for the establishment of an independent assessment of the release of fossil fuel CO_2 to the atmosphere at the regional to international level (Pacala et al., 2010). If only CO_2 concentrations are measured, it is usually very difficult to ascertain the specific source of CO_2, in part because the biosphere is a large and variable component. Fossil fuel ^{14}C provides a unique and exploitable tracer. In the most simple of mixing models between background (clean) air and a fossil fuel contribution, knowing atmospheric $^{14}CO_2$ to ≤ 2‰ equates to knowing the fossil fuel contribution to ≤ 2ppm (1-sigma) out of the present 380ppm. It is estimated that several thousand high-precision $^{14}CO_2$ analyses per year will be required to provide an independent seasonal estimate of North American (NA) fossil fuel emissions and reduce the uncertainty in the large-scale NA estimates. As individual regions and metropolitan areas independently enact cap and trade policies, the number of analyses and modeling rigor will increase.

The discrimination of fossil-fuel CO_2 emissions from natural exchanges of CO_2 (terrestrial and oceanic) is significantly aided by isotopic measurements of atmospheric CO_2 and measurements of other combustion tracers (e.g., CO, acetylene, benzene, *n*-pentanes, propane). Fossil-fuel carbon is devoid of ^{14}C (and also has a smaller $^{13}C/^{12}C$ ratio than atmospheric CO_2), which makes the $^{14}C/^{12}C$ ratio of atmospheric CO_2 susceptible to the emission of $CO_{2,ff}$ (fossil-fuel CO_2) because it increases ^{12}C without increasing ^{14}C. Between the beginning of the industrial revolution and atmospheric nuclear-weapons testing (which produced ^{14}C via n-p reactions), the $\Delta^{14}C$, i.e., the ratio of ^{14}C to ^{12}C, includes a correction for mass-dependent fractionation (Stuiver and Polach 1977) of atmospheric CO_2 decreased to the point where the atmosphere "looked" 200 years old (Figure 1) (*c.f.*, Suess 1955, Tans et al. 1979, Keeling 1979, Stuiver and Quay 1982). The decrease in the $^{14}C/^{12}C$ and $^{13}C/^{12}C$ ratio of atmospheric CO_2, referred to as the Suess Effect, can help discriminate sources of CO_2 (e.g., Graven et al. 2009, Levin et al. 2003, Turnbull et al. 2006, 2008, 2010; Vogel et al. 2010). Before the nuclear-testing moratorium, atmospheric weapons testing nearly doubled the amount of ^{14}C in the atmosphere. Air-sea CO_2 exchange and the uptake and respiration of terrestrial carbon has drawn down the $^{14}C/^{12}C$ ratio in the atmosphere from a bomb peak of ~ 1000 ‰ to ~ 45 ‰ today (*e.g.*, Levin et al. 2010, Graven et al. 2010, Turnbull et al. 2010). The time-history of bomb-^{14}C makes it a useful multi-decadal carbon cycle tracer: carbon that was photosynthetically fixed in the 1960s and 1970s and incorporated into multidecadal soil

carbon pools is now being heterotrophically respired (*c.f.*, Gaudinski et al. 2000, Harden et al. 2002, Trumbore 2000, Swanston et al. 2005, among many).

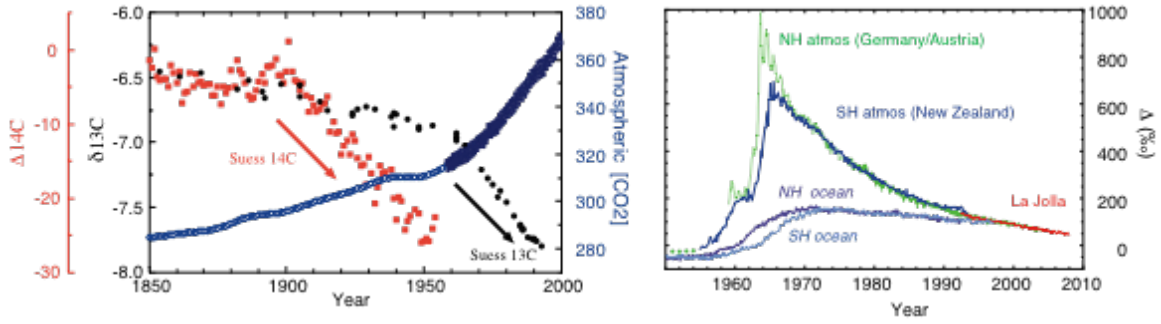

Figure 1. (Left) The influence of fossil-fuel CO_2 on atmospheric CO_2 and carbon isotopes. Post 1958 CO_2 data from Mauna Loa (Keeling and Whorf 2004, Keeling et al. 2010, Conway et al. 2010) and pre 1958 from firn air samples from Siple and Law Domes Antarctica (Etheridge et al. 1996, Francey et al. 1999, Friedli et al. 1986). Note that the Suess effect has a larger and faster impact on $\Delta^{14}C$ than $\delta^{13}C$. (Right) The "post-bomb" ^{14}C history in the atmosphere and surface ocean (data of Stuiver and Quay 1982; Levin et al. 2010; Manning and Meluish 1994; Graven et al. 2010; Guilderson et al. 2000; and Guilderson, unpublished). Atmospheric $\Delta^{14}C$ is an integration of unidirectional carbon (isotopic) fluxes between the atmosphere, ocean, and terrestrial biosphere, natural production in the stratosphere, and dilution due to the release of fossil fuel CO_2.

While other tracers, such as O_2/N_2 and $^{13}C/^{12}C$ ($\delta^{13}C$), are useful for distinguishing land versus oceanic components of the CO_2 variations, these tracers provide less useful information for distinguishing between land biospheric and fossil-fuel components. To quantify land biospheric exchange using inverse techniques based on O_2/N_2 or $^{13}C/^{12}C$ data, it is necessary to correct for the effects from fossil-fuel CO_2, which are assumed true and based on inventory products (e.g., Battle et al. 2000, Francey et al. 1995, Gurney et al. 2003, Patra et al. 2008, Rayner et al. 2002). *Note the strong corollary: the better one can uniquely and independently quantify the fossil-fuel component in a parcel of air the better one can determine the land biosphere flux using the aforementioned tracers.*

$\Delta^{14}C$ at clean air (background) sites is decreasing at an observed rate of ~ 5.5 ‰/yr (Levin et al. 2010, Graven et al. 2010, Turnbull et al. 2009). Box and global transport model-based trend analysis implies that the release of fossil fuel CO_2, if unbuffered by other processes, would decrease $\Delta^{14}C$ by ~15‰-yr^{-1} (Figure 2). Although carbon fluxes between the ocean and terrestrial biosphere are larger than those of fossil-fuel CO_2 emissions, the ^{14}C-isotopic signature yields gradients in excess of 15‰ downwind of sources (Figure 3). These gradients have been qualitatively reconstructed in the carbon fixed by annual plants (*e.g.,* Hsueh et al. 2007, Riley et al. 2008) and also via atmospheric transects (*e.g.,* Turnbull et al. 2008).

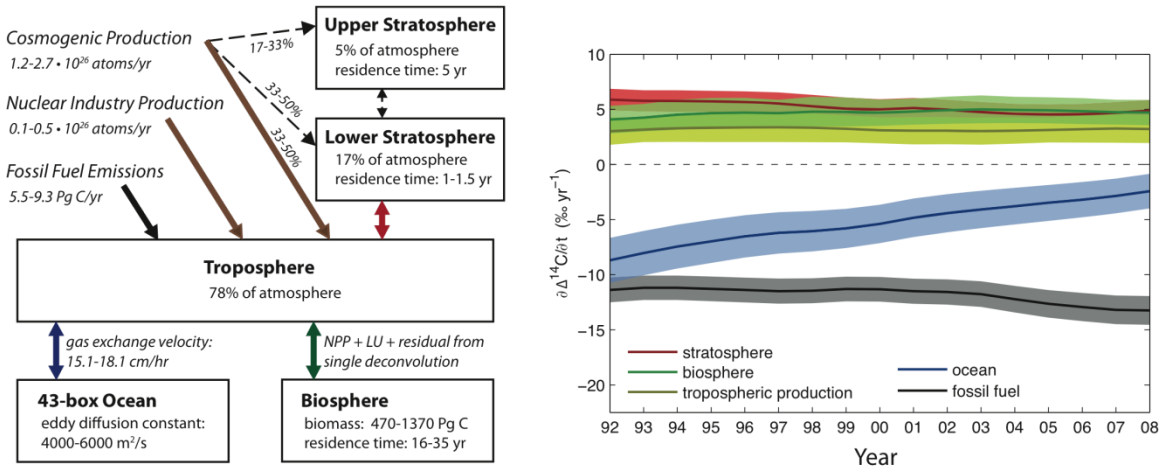

Figure 2. Box model based trend analysis on the influence of natural ^{14}C production, isotopic exchange and CO_2 fluxes between the atmosphere, ocean, and terrestrial biosphere, and the influence of the combustion of fossil fuel CO_2 (modified from Graven et al. 2010, courtesy of H. Graven).

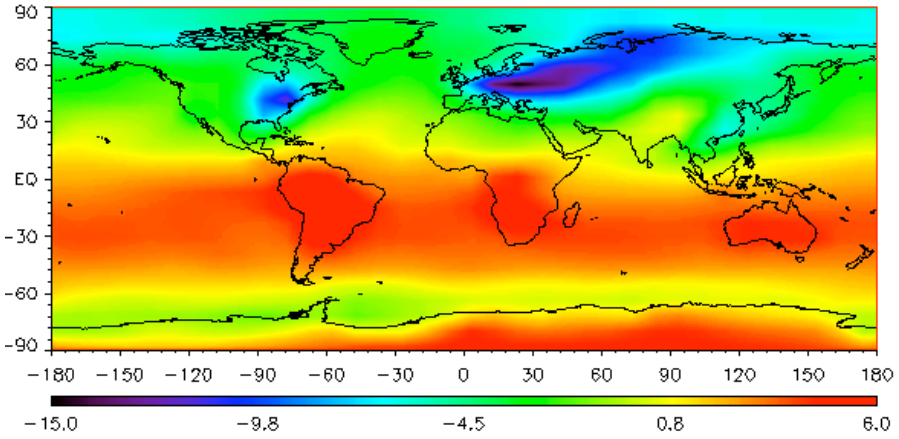

Figure 3. Simulated distribution of $\Delta^{14}C$ (‰) relative to the global mean in an ad-hoc, offline coupled carbon climate model including 2000 fossil fuel emissions (Randerson et al. 2002) image courtesy of JTR.

Due to the variability and complexity of atmospheric transport, an atmospheric modeling and retrieval system is required to determine the fossil fuel emission magnitude and distribution that give rise to the observed carbon dioxide concentrations and carbon isotope gradients (see Figure 3). The number of ^{14}C observations that might be possible in a fully-fledged carbon monitoring system for California (or the nation) is limited in part by cost and required infrastructure. Accordingly, a central challenge in this project was to develop an effective retrieval scheme using minimal observations, and develop methods to design observation network configurations. This work focused exclusively on designing a system for California as a test-bed. Fossil fuel CO_2 emissions account for ~96% of the total California anthropogenic CO_2 emissions (CEC GHG Inventory, 2006). The topographic complexity and challenging atmospheric transport variability over

California could be considered a near 'worse case scenario' for network optimization and retrieval design and provides a fundamental litmus test to the application of top down inversions and retrievals.

Model Descriptions

This work utilized the state-of-the-art, high-resolution Weather Research and Forecast model (WRF): WRF-ARM v3.1 (Skamarock et al., 2005; Skamarock and Klemp, 2008). We customized WRF to simulate the emissions and transport of multiple tagged tracers for use in our fossil fuel inversions. For our numerical experiments the WRF domain encompassed a rectangular region covering California and surrounding areas using grid-cells with a 12-15 km horizontal resolution, depending on the simulation. The vertical domain used a pressure-based coordinate system with multiple model levels in the boundary layer. The outer domain of the model was forced using meteorological data (including winds and temperatures) from the NCEP Eta North American Mesoscale (NAM) analysis with a 40 km resolution[1]. Simulations were conducted for winter and summer flow conditions in for January 2006 and July 2006 (Figure 4). No additional nudging or nesting was done.

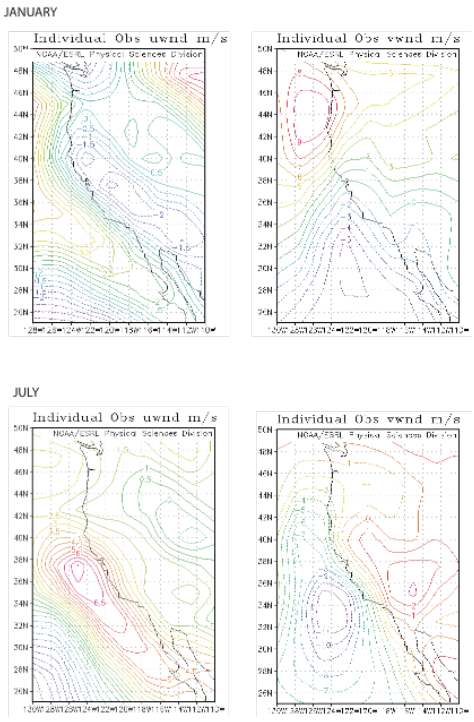

Figure 4. Average U and V zonal and meridional wind fields January and July 2006 used in the numerical experiments.

For transport of emissions into California from the rest of the world, we used the LLNL-IMPACT model (Rotman et al., 2004), with the Transcom-3 emission dataset (*c.f.*, Gurney et al., 2003; Law et al., 2006).

For the surface fossil fuel CO_2 emissions within California, we followed the spatial distribution of the California Air Resources Board (CARB) CO emissions, which are assessed within each geo-political air-basin (Figure 5) [www.carb.ca.gov]. We did this because at the time this project started, there was no standard fossil fuel CO_2 emission dataset of sufficient granularity. CO is monitored by CARB because it is a 'criteria pollutant' and has therefore been monitored in a regulatory and public health fashion, unlike CO_2. Since CO emissions are correlated with fossil fuel combustion, we scaled the CO emissions to generate CO_2 emissions, using simple linear scaling between the CO emissions and the CARB estimate of California's fossil fuel CO_2 emissions. We then aggregated the 16 CARB air-basins into 11-15 regions, depending on the simulation, to reduce the computational cost, and to avoid retrieval complications

[1] http://dss.ucar.edu/datasets/ds609.2/

that would arise when using regions of disparate size.

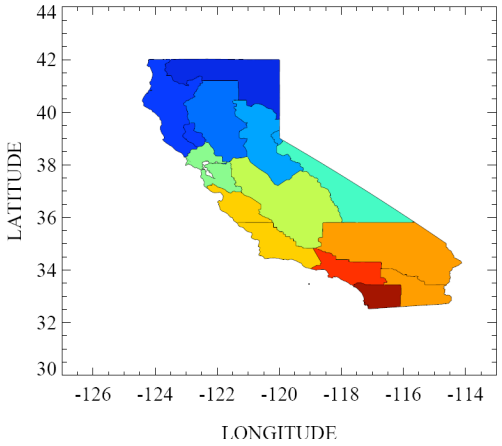

Figure 5: Our independent California emission regions, based on the air-basins defined by the California air resources board.

To illustrate the complex atmospheric transport, in Figure 6 we show the fossil fuel plumes from Los Angeles and San Francisco for two different weather patterns. A measurement made at any given location is clearly going to depend on the weather leading up to the measurement. Thus, in order to determine the GHG emissions from each region using *in situ* atmospheric measurements of those GHGs, it is necessary to use an atmospheric model to simulate the actual weather and transport. We used the LLNL-IMPACT model and the WRF-CHEM community model (both described above), with observed (aka assimilated) meteorology in order to recreate the actual transport that occurred.

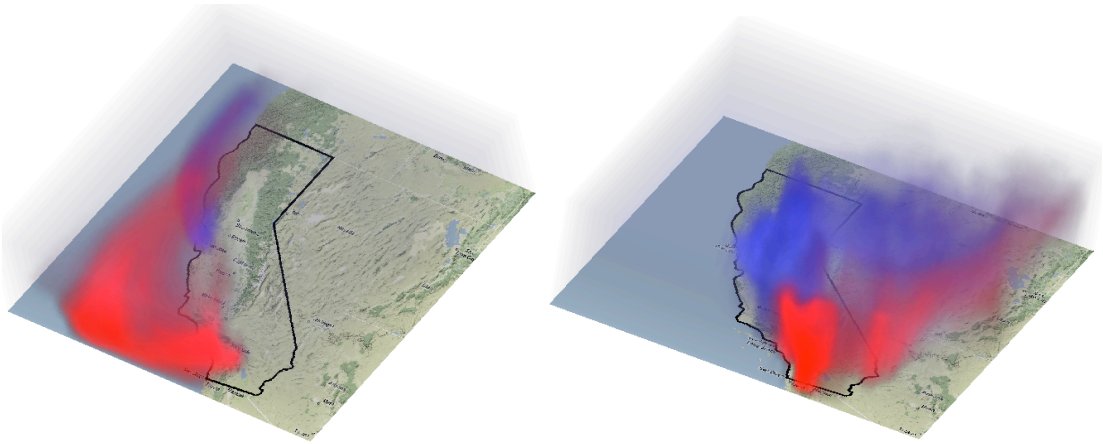

Figure 6: 3D images of fossil fuel plumes from Los Angeles (red) and San Francisco (blue) for two different weather patterns in January 2006, as generated by the WRF-CHEM model. The intensity of color is proportional to concentration. Note the strong offshore flow in the left-most panel due to strong Santa Ana winds.

The measured concentration of each tracer at a particular spatio-temporal location is a linear combination of the plumes from each region at that location (for non-reactive species such as CO_2). The inverse challenge is to calculate the emission strengths for

each region that best fit the observed concentrations. In general this is difficult because there are errors in the measurements and in the modeling of the plumes. We solve this inversion problem using the strategy illustrated in Figure 7.

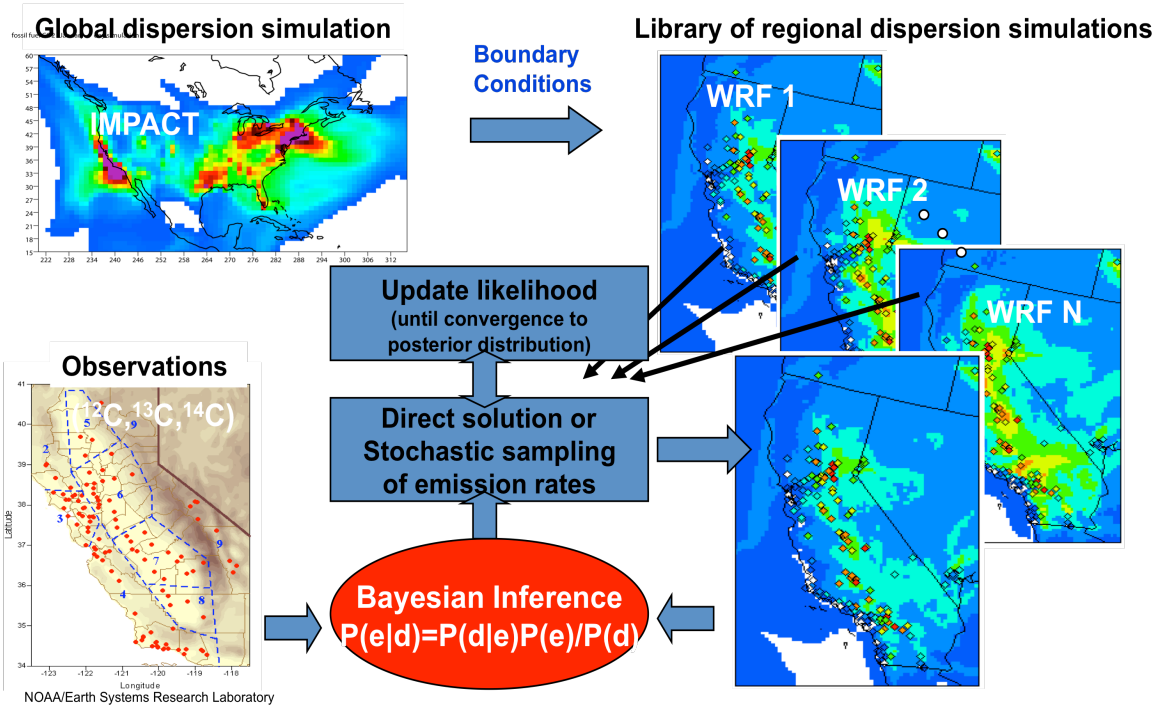

Figure 7. Symbolic representation of our inversion algorithm for retrieving regional emissions.

Inversions & Retrievals: The Bayesian Inference step combines the *a priori* estimates of the emissions, and their uncertainty, for each region with the results of the observations, and their uncertainty, and an ensemble of model predicted plumes for each region, and their uncertainty. The result is the mathematical best estimate of the emissions and their errors. In the case of non-linearities, or if we are using a statistical sampling technique such as a Markov Chain Monte Carlo technique, then the process is iterated until it converges (*i.e.,* reaches stationarity). For the Bayesian inference we can use both a direct inversion capability, which is fast but requires assumptions of linearity and Gaussianity of errors, or one of several statistical sampling techniques, which are computationally slower but do not require either linearity or Gaussianity (Chow, et al., 2008; Delle Monache, et al., 2008).

Up until our work, almost all emission inversions had been carried out under the assumption that all model errors are Gaussian and unbiased. We tested this assumption by running multiple configurations of WRF for 4 days (plus spin-up), then selecting one configuration to be the 'synthetic truth' and generating synthetic observations by sampling the synthetic truth at multiple locations and adding random unbiased noise to represent measurement uncertainty. We then used the other configurations to retrieve the emissions.

Intercomparison of the retrieved results in Figure 8 shows the errors induced in the retrieved emissions for Los Angeles by the model errors (the results for the other air-basins are similar). The posterior PDFs do not overlap, ie the retrieved estimates do not agree within their error uncertainties. This means that previous inversion studies are neglecting a major source of error. We can also see that the mean and uncertainty of the ensemble *does* match the synthetic truth within its uncertainty. Thus, the use of an ensemble of models should provide a better estimate of emission amplitude and uncertainty for any real observation network.

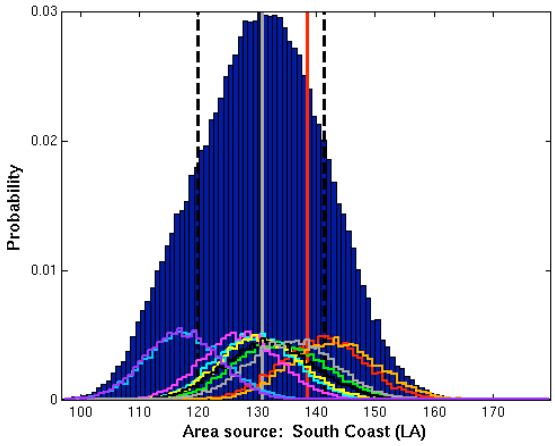

Figure 8. Each colored line shows the retrieved (a posteriori) probability density function (PDF) for fossil fuel CO_2 emissions from Los Angeles using synthetic data generated by a different model configuration. The solid blue area shows the combined a posteriori PDF from all the ensemble members. The gray and dashed lines show the median and one standard deviation of the a posteriori distribution, respectively. The red line shows the true synthetic value, which lies within the predicted range. These results were based on 4 days of simulated observations.

The main source of the variation between the different model configurations in Figure 8 arises from the uncertainty in the atmospheric boundary layer parameterization in the WRF model (Appendix Table 1). The alternative surface parameterizations were of secondary importance, and the alternative initial and boundary conditions were of least importance in this test.

Network design: The main goal of the network design analysis was to begin to determine the observing needs for constraining fossil fuel emissions in CA. A bare minimum of 15 observational data points are required to constrain the emissions from the 15 CARB basins (*i.e.* it is a linear system of 15 equations with 15 unknowns). In practice, however, many more observations are needed, because emissions inversion problems are ill-posed and ill-conditioned. Network design principles can be used to determine how these additional observations are collected (Gloor et al. 2000). One aspect of network design is to optimize the locations and frequency at which measurements are made. A hypothetical fossil fuel observing network clustered around the Los Angeles, for example, will have a difficult time constraining emissions from Northern California.

Optimal locations are found by calculating and ranking metrics of interest (*e.g.*, the root-mean-square residual difference for CA-level emissions) among a set of candidate sites. An example set of 'near-optimal' locations for a CA fossil fuel observing network is shown in Figure 9. It is important to stress that this set of locations is not universal; it depends on the flow conditions simulated (*e.g.*, January 2006), the transport model and physical parameterizations used (*i.e.,* WRF), and other factors. Further research would be

needed to determine a more robust set of fossil fuel observing sites in CA.

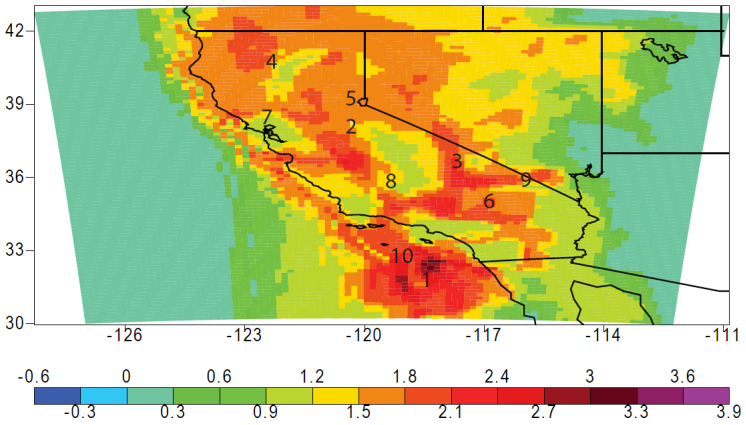

Figure 9. The colored surface shows the number of California air-basins constrained if the first observation site is in that location and it makes four measurements. The optimal location is noted by the number 1. Once that measurement site is located, subsequent optimal locations were calculated and noted by numbers 2 through 10. These 10 sites collectively constrain approximately 9 of the 11 air basin regions (assuming no model errors).

In addition to optimizing measurement locations, through this project we have also developed the capability to jointly optimize other factors important to designing fossil fuel observing networks. For example, we can consider measurement frequency, measurement costs, and other tracers besides CO_{2ff}. Simultaneously optimizing all of these factors, with or without constraints, is a difficult class of problems known as multi-objective optimization. We use genetic algorithms to search the vast design space for observing networks that optimize trade-offs among these factors. An example of a CA fossil fuel network design study we performed to demonstrate how to minimize inversion errors and measurement costs is shown in Figure 10. This shows that, unsurprisingly, under the assumptions of the problem, low inversion error solutions are associated with high costs, and vice versa. Our study also showed that networks with roughly similar costs and inversion errors may have vastly different spatial configurations.

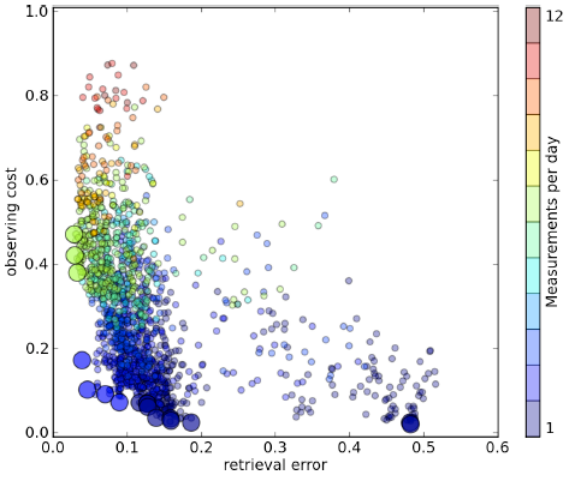

Figure 10. This figure illustrates the tradeoffs between two conflicting objectives (retrieval error and observing cost) in the design of an ff-CO_2 monitoring network. Each circle represents a configuration (sampling frequency and site locations) selected by an evolutionary algorithm, and the resulting retrieval error and observing cost for that configuration. Small circles are non-optimal solutions evaluated during the search phase. The large circles represent final optimal solutions. (Lucas et al., in prep).

Summary and Key findings:

1. An independent top-down retrieval of California fossil fuel CO_2 emissions appears to be a tractable problem: 15-20 sites are sufficient to overcome unbiased observational and modeling errors and constrain California emissions.

2. Performed similar inversion estimates using a network of opportunity based on FAA hazards (all above 200 m height). The results were almost as good as an optimally designed network.

3. Model biases in the transport and mixing, particularly that caused bythe behavior of the boundary layer (both diel and regionally due to topography) contribute large, poorly quantified uncertainties in retrieved emission estimates.

4. Assimilation of observations to constrain the uncertain processes in the atmospheric model (eg, boundary layer height) should significantly improve the retrieval.

5. Inclusion of a perturbed-physics ensemble of models can improve emission estimates, and better quantify the true uncertainty in those estimates.

6. An independent partitioning of fossil fuel CO_2 in air over California should provide a more accurate assessment of the net influence (ecosystem photosynthesis and respiration) of the terrestrial biosphere.

7. Additional tracers that are directly related to the production of CO_{2ff} (eg, carbon monoxide) could be calibrated against ^{14}C observations and included in the retrieval algorithm to increase the observational density.

Products

D. D. Lucas, P. Cameron-Smith, D. Bergmann, and T. Guilderson, 2011. Multiobjective network optimization for monitoring fossil fuel emissions in California. Manuscript in prep. *Geophys. Res. Letts.* LLNL-JRNL- 437391-DRAFT

D. D. Lucas, D. J. Bergmann, P. J. Cameron-Smith, E. Gard, T. P. Guilderson, D. Rotman and J. K. Stolaroff, 2010. Multi-objective design of optimal greenhouse gas observation networks, EOS Trans. AGU, GC13D-0729. LLNL-POST-463799

P. Cameron-Smith, B. Kosovic, T. Guilderson, L. Delle Monache, D. Bergmann, 2009. Fossil Fuel Emission Verification Modeling at LLNL. LLNL-TR-415915

L. Delle Monache, B. Kosovoic, P. Cameron-Smith, D. Bergmann, K. Grant, and T. Guilderson, 2008. Toward regional fossil fuel CO_2 emissions verification using WRF-CHEM. *EOS Trans. AGU*, A53H-03. LLNL-ABS-404201

B. Kosovic, L. Delle Monache, P. Cameron-Smith, D. Bergmann, K. Grant, and T. Guilderson, 2008. Toward regional fossil fuel CO_2 emissions verification using WRF-CHEM. *WRF Users Workshop*, June 23-27, 2008. Boulder CO. LLNL-ABS-404201

T.P. Guilderson, P. Cameron-Smith, B. Kosovic, D. L. Delle Monache, D. Bergmann, and K. Grant, 2008. Attribution of Carbon in the Atmosphere: A Fossil Fuel Emission Verification Capability and a Tool to Reduce the Uncertainties in the Carbon Budget. California Climate Change Conference, Sacramento CA. LLNL-ABS-406850

VIDEO: California Emission Flow Patterns. K. Grant et al., 2008 LLNL-VIDEO 402719

References

Battle, M., M. L. Bender, P. P. Tans, J.W.C. White, J. T. Ellis, T. Conway, and R. J. Francey, 2000, Global carbon sinks and their variability inferred from atmospheric O_2 and delta C-13, *Science*, vol. 287, pp. 2467-2470.

CEC GHG Inventory, 2006, California Climate Change Portal www.climatechange.ca.gov/inventory/index.html.

Chow, T., B. Kosovic, and S. Chan, 2008: Source inversion for contaminant plume dispersion in urban environments using building-resolving simulations. *J. Appl. Meteor. Climatol.,* 47, 1553–1572.

Conway, T. J., P. M. Lang, and K.A. Masarie, 2010, Atmospheric Carbon Dioxide Dry Air Mole Fractions from the NOAA ESRL Carbon Cycle Cooperative Global Air Sampling Network, 1968-2009 (www.esrl.noaa.gov/gmd/ccgg/trends/#mlo).

Delle Monache, L., et al., 2008, Bayesian Inference and Markov Chain Monte Carlo Sampling to Reconstruct a Contaminant Source on a Continental Scale. *J. Appl. Meteor. Climatol*., 47, 2600-2613.

Etheridge, D. M., et al., 1996, Natural and anthropogenic changes in atmospheric CO_2 over the last 1000 years from air in Antarctic ice and firn, *J. Geophys. Res.*, vol. 101, pp. 4115-4128.

Francey, R. J., P. P. Tans, and C. E. Allison, 1995, Changes in oceanic and terrestrial carbon uptake since 1982, *Nature*, vol. 373, pp. 326-330.

Francey, R. J., et al., 1999, A 1000-year high-precision record of $\delta^{13}C$ in atmospheric CO_2, *Tellus* B, vol. 51, pp. 170-193.

Friedli, H., H, Lötscher, H. Oeschger, U. Siegenthaler, and B. Stauffer, 1986, Ice record of the 13C/12C ratio of atmospheric CO2 in the past two centuries, *Nature*, vol. 324, pp. 237-238.

Gaudinski, J. B., S. E. Trumbore, E. A. Davidson, and S. Zheng, 2000, Soil carbon cycling in a temperate forest: radiocarbon-based estimates of residence times, sequestration rates and partitioning of fluxes, *Biogeochemistry*, vol. 51, pp. 33-69.

Gloor, M., S.-M. Fan, S. Pacala, and J. Sarmiento, 2000, Optimal sampling of the atmosphere for purpose of inverse modeling: A model study, Global Biogeochem. Cycles, vol. 14, pp. 407-428.

Graven, H. D., B. B. Stephens, T. P. Guilderson, T. L. Campos, D. S. Schimel, J. E. Campbell, and R. F. Keeling, 2009, Vertical profiles of biogenic and fossil-fuel-derived CO_2 from airborne measurements of $\Delta^{14}CO_2$ and CO_2 above Colorado, *Tellus B*, Mar 5 2009 DOI: 10.1111/j.1600-0889.2009.00421.x.

Graven, H. D., T. P. Guilderson, and R. F. Keeling, 2010, Observations of $\Delta^{14}C$ in CO_2 at La Jolla, California, USA 1992-2007, in revision*, J. Geophys. Res. Atmospheres.*

Guilderson, T. P., D. P. Schrag, E. Goddard, M. Kashgarian, G.M. Wellington, and B.K. Lindsey, 2000, Southwest subtropical Pacific surface water radiocarbon in a high-resolution coral record, *Radiocarbon,* vol. 42, pp. 249-256.

Gurney, K. R., et al., 2003, TransCom 3 CO_2 inversion intercomparison: 1. Annual mean control results and sensitivity to transport and prior flux information, *Tellus*, 55B, pp. 555-579.

Harden, J. W., T. L. Fries, and M. J. Pavich, 2002, Cycling of beryllium and carbon through hillslope soils in Iowa, *Biogeochemistry*, 60, pp 317-336.

Hsueh, D. Y., N. Y. Krakauer, J.T . Randerson, X. Xu, S. E. Trumbore, and J. R. Southon, 2007, Regional patterns of radiocarbon and fossil-fuel-derived CO_2 in surface air across North America, *Geophys. Res. Lett.,* 34, L02816, doi:10.1029/2006GL027032.

Keeling, C. D., 1979, The Suess Effect: ^{13}Carbon-^{14}Carbon Interrelations. *Environment International*, 2, pp. 229-300.

Keeling, C. D., and T. P. Whorf, 2004, Atmospheric CO_2 concentrations derived from flask air samples at sites in the SIO network, in *Trends: A Compendium of Data on Global Change*, Carbon Dioxide Information Analysis Center, Oak Ridge National Laboratory, U.S. Department of Energy, Oak Ridge, Tennessee, U.S.A.

Keeling, R. F., S. C. Piper, A. F. Bollenbacher, and S. J. Walker, 2010, Monthly atmospheric $^{13}C/^{12}C$ isotopic ratios for 11 SIO stations, in *Trends: A Compendium of Data on Global Change*, Carbon Dioxide Information Analysis Center, Oak Ridge National Laboratory, U.S. Department of Energy, Oak Ridge, Tennessee, U.S.A.

Law, R., W. Peters, and C. Rödenbeck, 2006, Protocol for TransCom continuous data experiment, Purdue Climate Change Res. Cent. Tech. Rep. (Available at www.purdue.edu/climate/publications/T3%5B1%5D.continuous.protocol_v6.pdf)

Levin, I., B. Kromer, M. Schmidt, and H. Sartorius, 2003, A novel approach for independent budgeting of fossil fuel CO2 over Europe by $^{14}CO_2$ observations. *Geophys. Res. Lett.* 30(23), pp. 2194-2198.

Manning, M. R., and W. H. Melhuish, 1994, Atmospheric $\Delta^{14}C$ record from Wellington, in: *Trends '93: A Compendium of Data on Global Change*, Publ. ORNL/CDIAC-65. edited by T. A. Boden et al., Carbon Dioxide Inf. Anal. Cent., Oak Ridge National Laboratory, Oak Ridge, Tennessee, pp. 193-202.

Pacala, S. W, et al., 2009, *Verifying Greenhouse Gas Emissions: Methods to Support International Climate Agreements,* National Academies Press, Washington DC, 130 pp.

Patra, P. K., et al., 2008, TransCom model simulations of hourly atmospheric CO_2: Analysis of synoptic-scale variations for the period 2002-2003. *Global Biogeochem. Cycles*, 22, GB4013, doi:10.1029/2007GB003081.

Randerson, J. T., I. G. Enting, E.A.G. Schuur, K. Caldeira, and I. Y. Fung, 2002, Seasonal and latitudinal variability of troposphere Delta(CO2)- C-14: Post bomb contributions from fossil fuels, oceans, the stratosphere, and the terrestrial biosphere, *Global Biogeochemical Cycles*, 16(4): art. no.-1112.

Rayner, P. J., I. G. Enting, R. J. Francey, and R. Langenfelds, 2002, Reconstructing the recent carbon cycle from atmospheric CO_2, $\delta^{13}C$ and O_2/N_2 observations, *Tellus B*, vol. 51, pp. 213-232.

Riley, W. J., et al., 2008, Where do fossil fuel carbon dioxide emissions from California go? An

analysis based on radiocarbon observations and an atmospheric transport model, *J. Geophys. Res.,* 113, G04002, doi:10.1029/2007JG00625.

Rotman, D.A. et al., 2004, IMPACT, the LLNL 3-D global atmospheric chemical transport model for the combined troposphere and stratosphere: Model description and analysis of ozone and other trace gases", *J. Geophys. Res.*, 9, D4, D04303 10.1029/2002JD003155.

Skamarock, W.C., et al., 2005, A description of the Advanced Research WRF Version 2, NCAR Technical Note NCAR/TN-468+STR.

Skamarock, W.C., and J.B. Klemp, 2008, A Time-Split Nonhydrostatic Atmospheric Model for Research and NWP Applications. *J. Comp. Phys*. 227,7, 3465-3485.

Stuiver, M., and H. A. Polach, 1977, Discussion: reporting of ^{14}C data, *Radiocarbon*, vol. 19, pp. 355-363.

Stuiver, M., and P. D. Quay, 1982, Atmospheric ^{14}C changes resulting from fossil fuel CO_2 release and cosmic ray variability, *Earth and Planet. Sci. Letts*., vol. 53, pp. 349-362.

Suess, H. E., Radiocarbon concentration in modern wood, 1955, *Science*, vol. 122, p. 415.

Swanston, C. W., M. S. Torn, P. J. Hanson, J. R. Southon, C. T. Garten, E. M. Hanlon, and L. Ganio, 2005, Initial characterization of process of soil carbon stabilization using forest stand-level radiocarbon enrichment, *Geoderma*, vol. 128, pp. 52-62.

Tans, P.P., A.F.M. de Jong and W.G. Mook, 1979, Natural atmospheric ^{14}C variation and the Suess effect, *Nature*, vol. 280, pp. 826.

Trumbore, S.E., 2000, Age of soil organic matter and soil respiration: Radiocarbon constraints on belowground C dynamics, *Ecological Applications,* vol. 10(2), pp. 399-411.

Turnbull, J. C., J. B. Miller, S. J. Lehman, P. P. Tans, R. J. Sparks, and J. Southon, 2006, Comparison of $^{14}CO_2$, CO, and SF_6 as tracers for recently added fossil fuel CO_2 in the atmosphere and implications for biological CO2 exchange, *Geophys. Res. Lett.,* 33, L01817, doi:10.1029/2005GL024213.

Turnbull, J. C., J. B. Miller, S. J.Lehman, D. Hurst, W. Peters, P. P.Tans, J. Southon, S. A. Montzka, J. W.Elkins, D. J.Mondeel, P. A. Romashkin, N. Elansky, and A. Skorokhod, 2009. Spatial distribution of 14CO2 across Eurasia: measurements from the TROICA-8 expedition, *Atmos. Chem. Phys*., vol. 9, pp. 175-187.

Turnbull, J. C. et al., 2010. Measurement of Fossil Fuel Derived Carbon Dioxide and Other Anthropogenic Trace Gases Above Sacramento, California in Spring 2009, *Atmos. Chem. Phys. Discuss*., vol. 10, pp. 21567-21613, doi:10.5194/acpd-10-2156702910.

Vogel, F. R., S. Hammer, A. Steinhof, B., Kromer, B. and I. Levin, 2010, Implication of weekly and diurnal ^{14}C calibration on hourly estimates of CO-based fossil fuel CO_2 at a moderately polluted site in southwestern Germany, *Tellus*, DOI: 10.1111/j.1600-0889.2010.00477.

Appendix Table 1: Parameterization schemes utilized in experiments and full retrievals

Ensemble used with Markov Chain Monte Carlo simulations:

Member # (color)	IC/BC	BL Scheme	Surface Scheme
1 (red)	AWIP	YSU	TDS
2 (green)	AWIP	YSU	NOAH
3 (orange)	AWIP	YSU	RUC
4 (cyan)	AWIP	MY	TDS
5 (magenta)	AWIP	MY	NOAH
6 (yellow)	AWIP	MY	RUC
7 (black)	FNL	YSU	TDS
8 (light blue)	FNL	MY	TDS
9 (gray)	NNRP	YSU	TDS
10 (purple)	NNRP	MY	TDS

The colors refer to the colors in figure 8.

Ensemble generated by our automatic ensemble simulation system:

Run	sf_surface_physics	bl_pbl_physics	cu_physics	sf_sfclay_physics
1	1	1	1	1
2	1	1	2	1
3	1	1	3	1
4	1	2	1	2
5	1	2	2	2
6	1	2	3	2
7	1	6	1	5
8	1	6	2	5
9	1	6	3	5
10	2	1	1	1
11	2	1	2	1
12	2	1	3	1
13	2	2	1	2
14	2	2	2	2
15	2	2	3	2
16	2	6	1	5
17	2	6	2	5
18	2	6	3	5
19	3	1	1	1
20	3	1	2	1
21	3	1	3	1
22	3	2	1	2
23	3	2	2	2
24	3	2	3	2
25	3	6	1	5
26	3	6	2	5
27	3	6	3	5

sf_surface_physics (land-surface option)
= 1, thermal diffusion scheme
= 2, unified Noah land-surface model
= 3, RUC land-surface model

bl_pbl_physics (boundary-layer option)
= 1, YSU scheme (use sf_sfclay_physics=1)
= 2, Mellor-Yamada-Janjic (Eta) TKE scheme (use sf_sfclay_physics=2)
= 6, MYNN 3rd level TKE (sf_sfclay_physics=5)

cu_physics (cumulus option)
= 1, Kain-Fritsch (new Eta) scheme
= 2, Betts-Miller-Janjic scheme
= 3, Grell-Devenyi ensemble scheme

sf_sfclay_physics (surface-layer option)
= 1, Monin-Obukhov scheme
= 2, Monin-Obukhov (Janjic Eta) scheme
= 5, MYNN